Brillouin scattering study of the structural phase transition in the two-layer orthorhombic form of $K_3Co(CN)_6$ single crystals

1991 J. Phys.: Condens. Matter 3 5171

(http://iopscience.iop.org/0953-8984/3/27/010)

J. Phys.: Condens. Matter 3 (1991) 5171–5182. Printed in the UK

Brillouin scattering study of the structural phase transition in the two-layer orthorhombic form of $K_3Co(CN)_6$ single crystals

Akira Yoshihara†, Tadao Fujimura† and Yoshiyuki Morioka‡

† Research Institute for Scientific Measurements, Tohoku University, Katahira 2-1-1, Aoba-ku, Sendai 980, Japan

‡ Department of Chemistry, Faculty of Science, Tohoku University, Aramaki Aza-Aoba, Aoba-ku, Sendai 980, Japan

Received 5 February 1991

Abstract. The second-order structural phase transition in the two-layer orthorhombic form of $K_3Co(CN)_6$ single crystals (D_{2h}^{14}–C_{2h}^5; $T_C \simeq 83.5$ K) is investigated through Brillouin scattering. A very-low-frequency soft optical phonon, which is the lowest soft optical phonon ever seen by light scattering techniques, has been observed. The soft phonon exhibits relaxational character as well as oscillatory character in the vicinity of the phase transition. Since the soft phonon belongs to the B_{3g} irreducible representation of the D_{2h} class, the C_{44} elastic constant is also expected to show softening. However, scattering from the C_{44} acoustic phonon is too weak to observe even near the phase transition. The [100] longitudinal acoustic phonon frequency shows a weak and continuous change through the phase transition. The behaviour can be reasonably explained by the Landau–Khalatnikov process with the dynamic susceptibility of the soft optical phonon.

1. Introduction

Potassium cobalticyanide ($K_3Co(CN)_6$) single crystals possess four different structural forms which are described by polytypic nomenclature as 1M (one-layer monoclinic), 20r (two-layer orthorhombic), 3M (three-layer monoclinic) and 7M (seven-layer monoclinic) (Kohn and Towns 1961). Among these crystal forms of $K_3Co(CN)_6$ the physical properties of the 1M and 20r forms have mainly been studied. Room-temperature crystal structures for the 1M form (C_{2h}^5 ($P2_1/c$); $z = 2$) and the 20r form (D_{2h}^{14} (Pnca); $z = 4$) have been determined by single-crystal x-ray diffraction (Figgis *et al* 1978). The 1M form crystal undergoes a non-ferric (constant rotational symmetry) second-order phase transition at $T_C \simeq 63$ K, induced by a Brillouin zone boundary soft phonon. The soft phonon is inevitably Raman inactive in the high-temperature phase but becomes Raman active in the low temperature phase (Saito *et al* 1984). The 20r form crystal also undergoes a second-order structural phase transition ($T_C \simeq 81$ K) which takes place at the Brillouin zone centre. A Raman-active soft optical phonon (B_{3g} symmetry of the point group D_{2h}) has been observed (Morioka and Nakagawa 1983). The crystal structures in the low-temperature phase are found to be C_{2h}^5 ($P2_1/n$) with $z = 4$ for these phase transitions (Morioka and Nakagawa 1983, Morioka *et al* 1985).

0953-8984/91/275171 + 12 $03.50

However, the unique twofold axis corresponds to the *b* axis for the 1M form ($P12_1/n1$ in the full notation), but the *a* axis for the 20r form ($P2_1/n11$). Raman scattering experiments successfully observed well defined soft phonons in both of the phase transitions (Morioka and Nakagawa 1983, Saito *et al* 1984). According to the lattice dynamical calculation for the 1M and 20r forms of $K_3Co(CN)_6$ the soft phonon in the 20r form can be regarded as the folding-back phonon of the Brillouin zone boundary soft phonon in the 1M form (Morioka 1986).

Now let us concentrate on the B_{3g} soft optical phonon in the 20r form crystal. The soft-phonon frequency at room temperature is about 16 cm^{-1} and decreases to about 3 cm^{-1} at 6 K above the phase transition (Morioka and Nakagawa 1983). However, the Raman study could not observe the soft phonon within several kelvins around the phase transition because of a strong Rayleigh peak. The details of the soft-phonon behaviour in the vicinity of the phase transition has not been fully elucidated. Note that the frequency region below 3 cm^{-1} can be precisely studied by means of the Fabry–Pérot spectroscopy known as Brillouin scattering. There are two reasons why we study the D_{2h}–C_{2h} phase transition in the 20r form of $K_3Co(CN)_6$ by means of Brillouin scattering. First of all, it is very interesting to study the dynamical behaviour of the very-low-frequency soft optical phonon near the second-order phase transition. To the best of our knowledge, only one example of a Brillouin scattering study of the soft optical phonon has been reported on the monoclinic–monoclinic isostructural phase transition in the molecular crystal $C_6Cl_4O_2$ known as chloranil (Girard *et al* 1982). However, the soft phonon is a Brillouin zone boundary phonon in the high-temperature phase and the Brillouin scattering study is inevitably limited to only a few kelvins below the phase transition temperature. Therefore the 20r form of $K_3Co(CN)_6$ single crystals can be a rare and unique example of Brillouin scattering study of a soft optical phonon. Secondly, according to group theoretical analysis, a bilinear coupling between the B_{3g} soft optical phonon and a shear elastic strain e_{YZ} (e_4) is allowed in the Landau free energy. This means that one can expect to observe the C_{44} soft acoustic phonon as well as the soft optical phonon by Brillouin scattering. Furthermore, since the soft-phonon frequency becomes extremely low near the phase transition, we might be able to see dynamical crossover effect between the soft optical phonon and the C_{44} acoustic phonon near the phase transition (Cummins 1979).

This is the first complete report on a Brillouin scattering study of the soft optical phonon through a second-order structural phase transition which takes place at the Brillouin zone centre.

2. Experimental details

The starting materials for $K_3Co(CN)_6$ single crystals were KCN and $CoCl_2 \cdot 6H_2O$, both reagent-grade chemicals. After synthesis and purification procedures, we obtained polycrystals of $K_3Co(CN)_6$. Single crystals were grown from saturated aqueous solutions by slow cooling. The polytypes of the obtained crystals can be easily distinguished by measuring the Raman spectrum at room temperature. For the 20r form crystals, a Raman line appears at around 16 cm^{-1}, which is the soft phonon, but not for the other forms of the crystals. Although the large 1M form crystals of excellent optical quality for light scattering experiment can be readily grown, it is very difficult to grow the 20r form crystals with an excellent optical quality. Sometimes, because of mixtures of $K_3Co_{1-x}Fe_x(CN)_6$ ($x \leq 0.03$) or rapid cooling the 20r form single crystals are accidentally

grown. After a large number of attempts, we obtained a couple of transparent platelets about 1.5 × 3.5 mm × 5 mm in size with faces perpendicular to the crystallographic two-fold axes. In this report, we adopt the X, Y, Z notation for the two-fold axes instead of the a, b, c notation.

Brillouin spectra were excited by 514.5 nm light from an Ar^+ laser in a single-cavity mode with a power of less than 50 mW at the sample. Because of the limited dimensions of the single crystals obtained, we mainly employed back-scattering geometries. Brillouin spectra were obtained using a laboratory-built piezoelectrically scanned five-pass Fabry–Pérot interferometer followed by photon-counting electronics and a computer-based data acquisition system (Haneda *et al* 1988, Yoshihara *et al* 1989a). Several free spectral ranges between 0.5 and 12 cm^{-1} with a finesse of about 60 and a contrast of about 10^{10} were employed. Oriented samples are affixed to a copper block using GE varnish 7031 and placed in a laboratory-built metal cryostat (Yoshihara *et al* 1990). The temperature of the sample is controlled with a proportional controller with a copper–constantan thermocouple and measured with a calibrated platinum resistance thermometer which is placed just behind the sample. Temperature fluctuations and drift are less than ±0.03 K for a data accumulation time of 1–10 min.

3. Results and discussion

3.1. Optical soft phonon

Examples of the temperature dependences of the soft-optical-phonon spectra around the phase transition are shown in figure 1. These spectra were observed in $X(Z, Y) - X$ scattering geometry, which allows one to observe the B_{3g} symmetry Raman-active phonons. The free spectral range was set to 9.73 ± 0.05 cm^{-1}. Below 85 K, the soft-phonon peak is absorbed into the Rayleigh wing and can no longer be observed in the spectra. In order to elucidate the soft-phonon behaviour near the phase transition, measurements with a much higher resolving power (narrower free spectral ranges) should be carried out. Figures 2(a) and 2(b) show the temperature development of the high-resolution soft-phonon spectra in the vicinity of the phase transition. The scattering geometry was $X(Z, Y + Z) - X$ and the free spectral range was set to 2.30 ± 0.01 cm^{-1} for figure 2(a) and 6.47 ± 0.03 cm^{-1} for figure 2(b). In spite of the narrower free spectral ranges employed, we could not observe the soft-phonon peak in a temperature range between 85 and 82 K but merely observed a broad structure around the elastic Rayleigh peak as shown in figures 2(a) and 2(b). Sharp peaks, which appear around ±0.7 cm^{-1}, are scattering from the longitudinal acoustic (LA) phonon propagating along the [100] direction. Thermal hysteresis of the transition temperature has not been detected within the experimental accuracy of our temperature measurement, ±0.1 K.

In order to determine the frequency shift and the width of the soft phonon, we need to assume lineshape functions for the Rayleigh and soft-phonon peaks. The lineshape function for the sharp Rayleigh peak (instrumental function) observed with a five-pass Fabry–Pérot interferometer is well established and given by (Lindsay *et al* 1977)

$$S_R(\omega) = I_R[\gamma^2/(\omega^2 + \gamma^2)]^5. \tag{1}$$

Then the true width of the Rayleigh peak (HWHM) is given by $(2^{1/5} - 1)^{1/2}\gamma$. Next we assume the damped harmonic oscillator response function for the soft phonon to be

$$S_{PH}(\omega) \sim [1 + n(\omega)]\,\mathrm{Im}(\omega_\infty^2 - \omega^2 - 2i\omega\Gamma)^{-1} \tag{2}$$

in which $n(\omega)$ is the Bose–Einstein factor, and ω_∞ and Γ are the frequency and the width

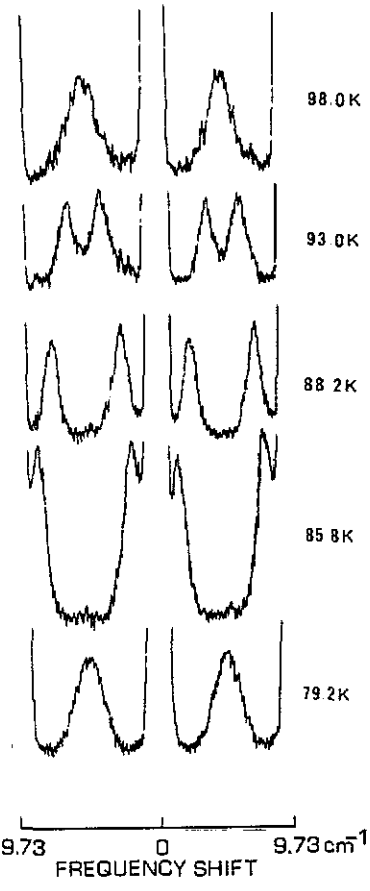

Figure 1. Temperature development of the soft-optical-phonon spectrum through the phase transition. The scattering geometry employed was $X(Z, Y) - X$ and the free spectral range was set to 9.73 cm^{-1}.

of the soft phonon. Following the deconvolution technique (Lindsay *et al* 1977), we can obtain an analytical expression for the deconvoluted spectrum using equations (1) and (2). Unfortunately the expression is too complicated to use, even for the simple response function. However, when the soft-phonon width Γ is larger than the width γ in equation (1) by a factor of about 5, the damped harmonic oscillator response function gives a reasonable fit to the observed spectrum as shown in figure 2(*b*) by full circles (see the 83.6 K spectrum). Note that the γ/Γ ratio strongly depends on a value of the free spectral range and it becomes larger for narrower free spectral ranges. We found that the response function can reasonably reproduce the observed spectra except for the highest-resolution spectra near the phase transition which are shown in figure 2(*a*). In these spectra, a broad structure, which cannot be reproduced by the simple damped harmonic oscillator response function, clearly appears around the elastic Rayleigh peak. In order to reproduce the observed spectra, we have phenomenologically introduced the oscillator–'relaxator' coupled response function, which is given by (Shapiro *et al* 1972)

$$S_{\mathrm{PH}}(\omega) \sim [1 + n(\omega)]\,\mathrm{Im}[\omega_\infty^2 - \omega^2 - 2\mathrm{i}\omega\Gamma - \delta^2/(1 - \mathrm{i}\omega\tau)]^{-1} \qquad (3)$$

in which $n(\omega)$ is the Bose–Einstein factor, τ is the relaxation time of the relaxation mode and δ is a coupling constant between the soft phonon and the relaxation mode. In this model, the optical phonon instability takes place at a temperature which satisfies

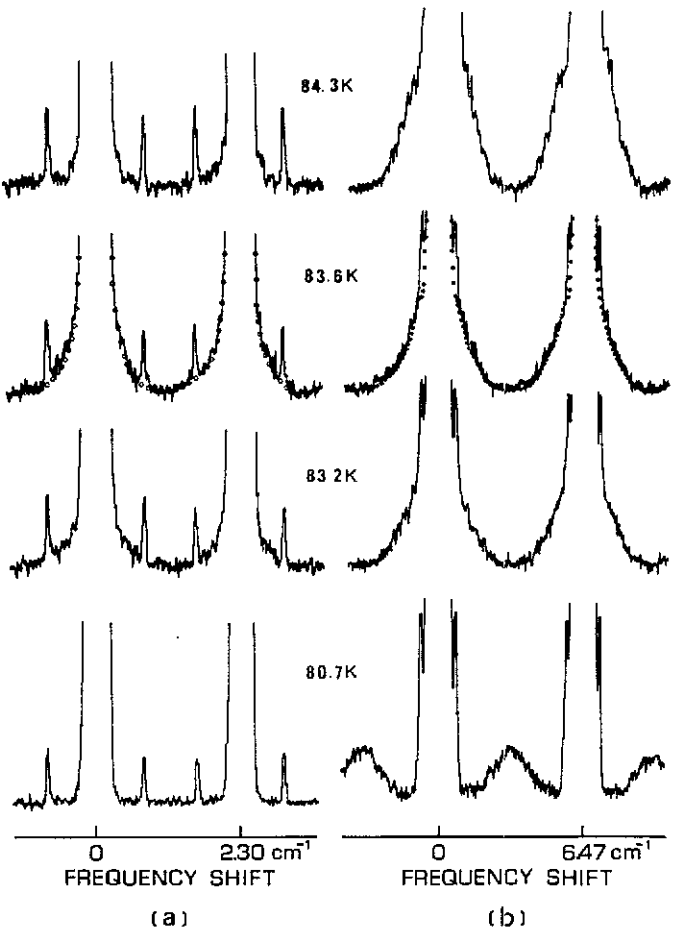

Figure 2. Temperature development of the high-resolution soft-phonon spectrum in the vicinity of the phase transition, observed in the $X(Z, Y+Z)-X$ scattering geometry, where the sharp peaks appearing at about ± 0.7 cm^{-1} are due to scattering from the [100] LA phonon: ●, in (*b*) 83.6 K spectrum calculated using the damped harmonic oscillator model (see equation (2)); ○, in (*a*) 83.6 K spectrum calculated using the soft-phonon–relaxator coupled model (see equation (3)).

$\omega_0^2 = \omega_\infty^2 - \delta^2 = 0$ instead of $\omega_{00}^2 = 0$. Using the response function, we tried to analyse the highest-resolution spectra near the phase transition. For example, when we choose $1/2\pi\tau = 0.43 \pm 0.02$ cm^{-1}, $\delta/2\pi = 0.25 \pm 0.01$ cm^{-1}, $\omega_{00}/2\pi = 1.40$ cm^{-1} and $\Gamma/2\pi = 0.7$ cm^{-1} for the 83.6 K spectrum, we can fully reproduce the observed spectra as shown by open circles. Figure 3 presents the soft-phonon frequency and the width as functions of temperature. The transition temperature T_C is found to be 83.5 ± 0.1 K. It is clear that the phonon width is about 0.7 cm^{-1} and almost independent of temperature in the high-temperature phase. However, the width exhibits a broad peak below T_C. A simple quasi-harmonic theory for the soft phonon cannot explain the behaviour. The relaxation time τ and the coupling constant δ are almost independent of temperature through the phase transition. The relaxational mode plays important roles within a few kelvins around the phase transition. The open triangles are the Raman scattering results

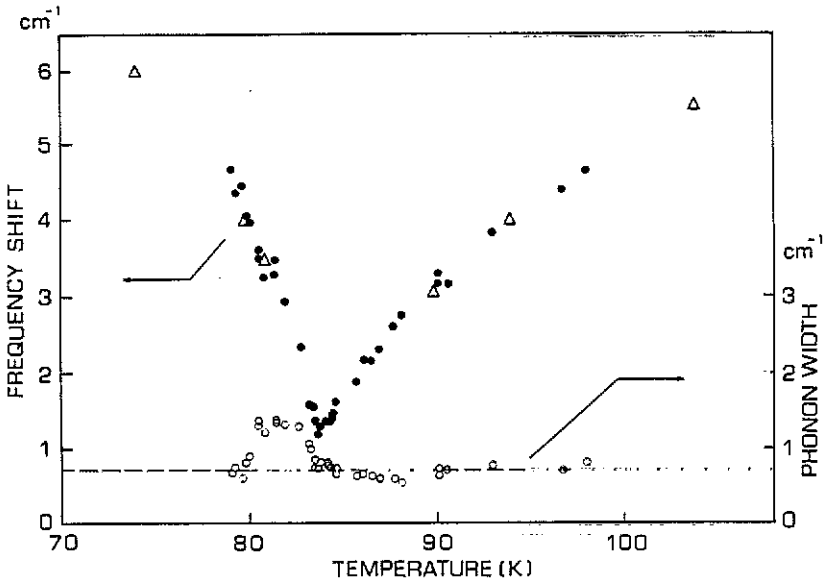

Figure 3. Temperature dependence of the soft-phonon frequency ω_{00} (●) and the phonon width Γ (○): △, the soft-phonon frequency determined by Raman scattering (Morioka and Nakagawa 1983); ———, [100] LA phonon frequency as a function of temperature.

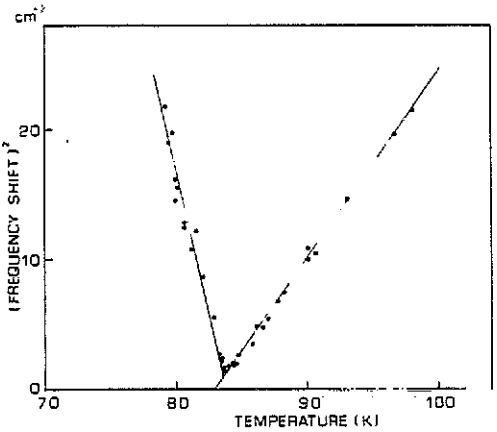

Figure 4. Square of the soft-phonon frequency as a function of temperature: ———, temperature dependences given by equations (4) and (5).

(Morioka and Nakagawa 1983). The transition temperature was found to be about 81 K. When the transition temperature is adjusted to the present value of 83.5 K, agreement between the Raman and Brillouin scattering results is excellent. Figure 4 shows the square of the phonon frequency as a function of temperature. It is evident that the squared frequency follows the linear temperature dependence as expected from the mean-field soft-phonon theory (Blinc and Zeks 1974) except in the close vicinity of the phase transition. The squared soft-phonon frequencies as a function of temperature are summarized as follows:

$$(\Delta n)^2 = \begin{cases} 1.4(T - 83.0)\ (\mathrm{cm}^{-1})^2 & \text{for } T > T_C \quad (4) \\ 4.5(83.6 - T)\ (\mathrm{cm}^{-1})^2 & \text{for } T < T_C. \quad (5) \end{cases}$$

From equation (4) and the $\delta/2\pi$-parameter already discussed, we find that $\omega_{00}^2 \simeq \omega_0^2$. Note that the ratio between the temperature coefficients in equations (3) and (4) is almost 3 and different from the mean-field value of 2. The calculated soft-phonon frequencies at 290 K and $T_C = 60$ K obtained using equations (4) and (5) are 17.0 cm^{-1} and 16.4 cm^{-1} and show reasonable agreement with the Raman results, 16 cm^{-1} and 15 cm^{-1}, respectively.

It is clear that we need to introduce the relaxational character for the soft optical phonon in the vicinity of the phase transition in order to reproduce the observed spectra. However, the physical origin of the relaxation mode is not understood yet and is left for future studies.

3.2. Acoustic phonons

First of all, let us start by discussing the C_{44} transverse acoustic (TA) phonon. According to the group theoretical analysis, one can expect a bilinear coupling term between the B_{3g} soft optical phonon and the shear strain e_{YZ} (e_4) in a simplified Landau free energy given by

$$F = \tfrac{1}{2}\alpha(T)Q^2 + \tfrac{1}{4}\beta Q^4 + \tfrac{1}{2}C_{44}^{(0)}e_4^2 + AQe_4. \quad (6)$$

Here $\alpha(T) = \alpha_0(T - T_0)$ and $\beta > 0$. Then the C_{44} elastic anomalies can be readily obtained through the standard calculation techniques (Rehwald 1973) as

$$C_{44} = \begin{cases} C_{44}^{(0)}(T - T_C)/(T - T_0) & \text{for } T > T_C \quad (7) \\ C_{44}^{(0)}(T_C - T)/(T_1 - T) & \text{for } T_C < T \quad (8) \end{cases}$$

in which $T_C = T_0 + A^2/C_{44}^{(0)}\alpha_0$ and $T_1 = T_C + (T_C - T_0)/2$. The phase transition is induced by the C_{44} acoustic instability prior to the optical phonon instability. According to the selection rules for the right-angle Brillouin scattering on the D_{2h} class (Vacher and Boyer 1972), the C_{44} acoustic phonon can be observed in the $X + Y[Z, X + Y]X - Y$ and $X + Z[Y, X + Z]X - Z$ types of scattering geometry. In both geometries, scattering intensity is governed by the Pockel's photoacoustic constant P_{44}. Because of the limited dimensions of the grown crystals (platelets in the Y–Z plane), we could scarcely prepare a thin sample for the C_{44} soft-phonon study in the latter scattering geometry. The Brillouin scattering intensity from the C_{44} acoustic phonon at temperature T is essentially given by

$$I_B \sim T(P_{44})^2/C_{44}. \quad (9)$$

If we assume that the phase transition is actually induced by the C_{44} acoustic instability, we can determine the two characteristic temperatures which appear in equation (7) as $T_C = 83.5$ K and $T_0 = 83.0$ K. Numerical calculation using equation (7) with these temperatures shows that the softening of the C_{44} acoustic phonon frequency and the enhancement of the scattering intensity becomes remarkable within only a few kelvins above T_C. Keeping these results in mind, we carefully examined scattering from the C_{44} TA phonon in a wide temperature range between 78 and 300 K, and with special attention near the phase transition, with the narrowest free spectral range 15 GHz. However, we could not observe scattering from the TA phonon even near the phase transition. This

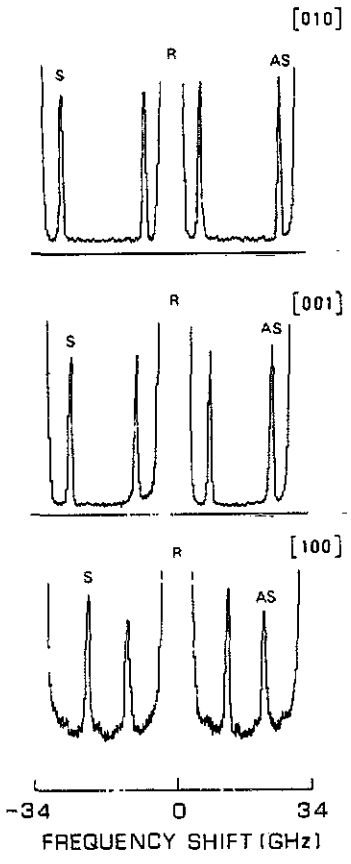

Figure 5. Brillouin spectra due to the LA phonons near the phase transition ($T = 83.7\ \mathrm{K} \simeq T_C + 0.2\ \mathrm{K}$): R, the Rayleigh peak; S, the Stokes component; AS the anti-Stokes component. These spectra were recorded for the same time (100 s) and are shown in the same vertical scale. Since the free spectral range is 34 GHz, the LA peaks overlap from different orders.

result seems to suggest that the P_{44} constant may be extremely small. In this case, Brillouin scattering might not be a suitable technique to study the C_{44} instability of $K_3Co(CN)_6$ and we should employ the ultrasonic pulse technique or the neutron inelastic scattering technique.

Next we discuss LA phonons. Examples of back-scattering Brillouin spectra due to the LA phonons, which propagate along the twofold axes, just above the transition temperature (about $T_C + 0.2$ K) are shown in figure 5. Vertical scales are common for these spectra. The data accumulation time was 100 s. According to the selection rules of Brillouin scattering by acoustic phonons (Vacher and Boyer 1972), which are propagating along the twofold axes of D_{2h} class, one can only observe scattering from the LA phonons in the back-scattering geometries. It is interesting to note the background levels in these spectra. The [100] phonon spectrum, which was measured in the same $X(Z, Y + Z) - X$ scattering geometry as used for the soft-optical-phonon study, clearly shows a very high background level which is due to the soft optical phonon. Figure 6 presents the LA phonon frequencies as a function of temperature around the phase transition. As can be seen from this figure, the [001] LA phonon frequency does not show an anomaly through the phase transition. The [010] LA phonon frequency shows a small scatter just below the transition temperature. This may be due to the domain wall motion. On the other hand, the [100] LA phonon frequency exhibits small but continuous behaviour through the phase transition. According to the group theoretical analysis, the

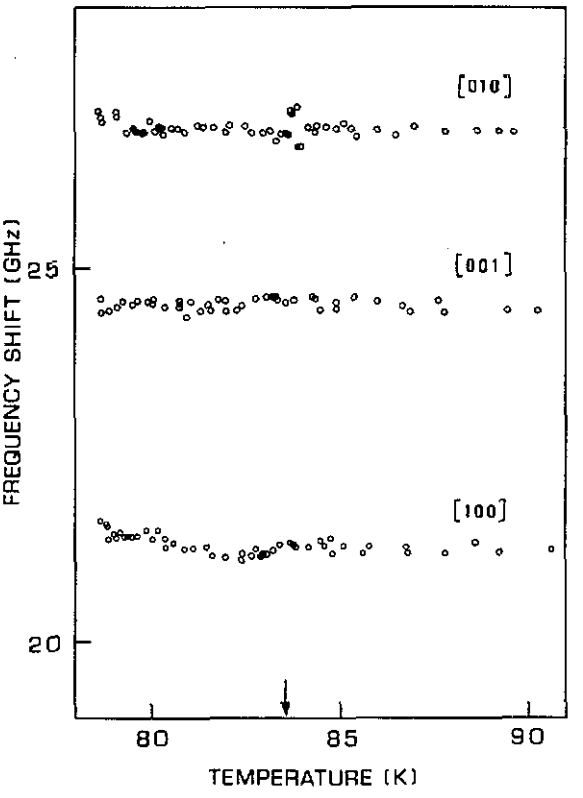

Figure 6. The LA phonon frequencies as a function of temperature for the back-scattering geometries. The phonon propagation directions are also given in this figure. The arrow indicates the transition temperature (T_C = 83.5 K).

lowest-order coupling between the longitudinal strain e_1 (A_g symmetry) and the order parameter (B_{3g} symmetry) is given by

$$F_{int} = Be_1Q^2. \tag{10}$$

Through the standard calculation technique (Rehwald 1973), one obtains a step function anomaly

$$\Delta C_{11} = C_{11}(T > T_C) - C_{11}(T < T_C) = 2B^2/\beta \tag{11}$$

at the transition temperature. Here the C_{11} elastic constant is related to Brillouin shift through the well known formula (Chandrasecharan 1951)

$$C_{11} = \rho V_{[100]}^2 = \rho\{\lambda_0 \Delta\nu_{B[100]}/[2n \sin(\theta_s/2)]\}^2 \tag{12}$$

in which $V_{[100]}$ is the velocity of sound along the [100] direction, ρ is the crystal density, λ_0 (=514.5 nm) is the wavelength of incident light in vacuum, n is the refractive index for incident light and θ_s is the scattering angle ($\theta_s = \pi$). Note that equation (12) is only correct for the LA phonon (Vacher and Boyer 1972). Clearly equation (11) cannot explain the observed anomaly. We sometimes observe a smooth and continuous change in the elastic constant through the second-order phase transition with linear strain–

quadratic order parameter couplings in the high-temperature phase by Brillouin scattering (Yoshihara *et al* 1984, 1985, 1989b). This behaviour can be understood by a Landau–Khalatnikov process. With the inclusion of this process, the elastic anomaly given by equation (11) should be replaced by

$$\Delta C_{11}(\omega) = 4B^2 Q_s^2 \chi_Q(\omega) = 4B^2 Q_s^2 \chi_Q(0)[\chi_Q(\omega)/\chi_Q(0)]. \tag{13}$$

Q_s is the spontaneous value of the order parameter, and $\chi_Q(\omega)$ and $\chi_Q(0)$ are the dynamic and static susceptibilities of the order parameter in the low-temperature phase. According to the thermodynamical treatment, the $4B^2 Q_s^2 \chi_Q(0)$ part should be replaced by $2B^2/\beta$. The real part of $\chi_Q(\omega)$ gives the frequency-dependent elastic constant and the imaginary part gives the line broadening of the Brillouin peak. Since we have not observed a line-broadening effect in our Brillouin spectrum, we only discuss the contribution from the real part of $\chi_Q(\omega)$. We should use the dynamic susceptibility for the phonon–'relaxator' oscillator coupled mode,

$$\mathrm{Re}\{\chi_Q(\omega_B/\chi_Q(0)\} = \omega_0^2[\omega_\infty^2 - \delta^2/(1 + \omega_B^2\tau^2) - \omega_B^2]$$

$$\times \{[\omega_{00}^2 - \delta^2/(1 + \omega_B^2\tau^2) - \omega_B^2]^2 + \omega_B^2[2\Gamma + \tau\delta^2/(1 + \omega_B^2\tau^2)]^2\}^{-1} \tag{14}$$

in which $\omega_B = 2\pi n_B$ ($n_B \simeq 0.713\,\mathrm{cm}^{-1}$) and $\omega_0^2 = \omega_\infty^2 - \delta^2$. Since the temperature dependences of the soft-optical-phonon parameters have been already determined, we can directly calculate the elastic anomaly using equations (12)–(14). However, we have no data on the index of refraction and the crystal density for this crystal to hand. We just calculate the squared Brillouin shift which is proportional to the elastic constant. Figure 7 shows the calculated elastic anomaly compared with the experimental results. In order to determine the magnitude of the step anomaly at T_C, which corresponds to the factor $4B^2 Q_s^2 \chi_Q(0)$ in equation (13), we assumed a linear temperature dependence for the normal part of the C_{11} elastic constants above and below T_C. Then we obtained a value of about 17 for the factor $4B^2 Q_s^2 \chi_Q(0)$ in our units of gigahertz squared. We should emphasize the fact that, once we determine the factor $4B^2 Q_s^2 \chi_Q(0)$ at T_C, there is no adjustable parameter in the calculation. When we take this into account, agreement between the calculation and the experimental data seems to be reasonable. Here, we want to make a comment. The dynamic susceptibility contains a contribution from the relaxator in the vicinity of the phase transition. However, we found that the relaxator does not contribute to the elastic anomaly. In fact we obtain the same result even for null coupling ($\delta = 0$) between the soft phonon and the relaxational mode in equation (14). The elastic anomaly stems from the Landau–Khalatnikov process due to the nearly overdamped soft-optical-phonon mode but not the relaxation mode.

4. Conclusion

The two-layer orthorhombic form of $K_3Co(CN)_6$ single crystals undergoes a typical second-order structural phase transition which is induced by a Raman-active soft optical phonon at the Brillouin zone centre. The temperature dependences of the soft-phonon frequency and the width around the phase transition were extensively studied by means of Brillouin scattering. The square of the soft-phonon frequency obeys the linear temperature dependence as expected from the classical mean-field theory above and below T_C. This is the lowest soft optical phonon ever observed by light scattering experiments.

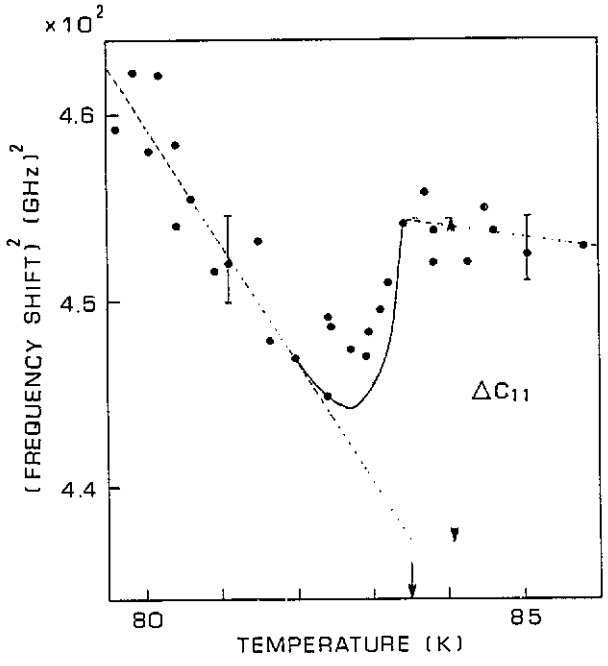

Figure 7. Comparison between the Landau–Khalatnikov contribution to the elastic anomaly and the observed contribution: ———, normal part of the C_{11} elastic constant (square of the [100] LA phonon frequency). In the low-temperature phase, it is given by $437 + 6.3 \times (83.5 - T)$ $(GHz)^2$. The arrow indicates the transition temperature (T_C = 83.5 K).

The soft phonon is not a simple damped harmonic oscillator but exhibits a relaxational character in the vicinity of the phase transition. However, the physical origin of the relaxation mode is not understood yet and is left for future studies.

The LA phonon propagating along the [100] axis shows a weak and continuous elastic anomaly at the phase transition. The elastic behaviour can be reasonably explained by linear strain–quadratic order parameter coupling with the dynamic susceptibility of the soft optical phonon. Since the soft phonon belongs to the one-dimensional B_{3g} irreducible representation of D_{2h} class, softening of the C_{44} elastic constant is expected. However, we could not observe scattering from the C_{44} acoustic phonon even near the phase transition in our Brillouin spectrum. Of course, this does not deny the possibility that the C_{44} soft acoustic phonon exists but it means that Brillouin scattering might not be a suitable technique for studying the C_{44} soft acoustic phonon for the 20r form $K_3Co(CN)_6$ crystal because of an extremely weak scattering intensity. In order to examine the possibility of the C_{44} soft acoustic phonon, ultrasonic or neutron inelastic scattering studies are strongly recommended.

Acknowledgments

One of the authors (AY) would like to thank Dr M Kataoka of the Institute for Materials Research, Tohoku University, for valuable discussions. This work is partly supported by a Grant-in-Aid from the Ministry of Education, Science and Culture of Japan.

References

Blinc R and Zeks B 1974 *Soft Modes in Ferroelectrics and Antiferroelectrics* (New York: Elsevier) ch 4
Chandrasecharan V 1951 *Proc. Indian Acad. Sci.* A **33** 183
Cummins H Z 1979 *Phil. Trans. R. Soc.* A **293** 393
Figgis B N, Skelton B W and White A H 1978 *Aust. J. Chem.* **31** 1195
Girard A, Delugeard Y, Ecolivet C and Cailleau H 1982 *J. Phys. C: Solid State Phys.* **15** 2127
Haneda Y, Yoshihara A, Sugawara T, Sasaki M, Takahashi K, Suzuki M, Takahashi A and Fujimura T 1988 *Bull. Res. Inst. Sci. Meas. Tohoku Univ.* **37** 215 (in Japanese), and references therein
Kohn J A and Towns W D 1961 *Acta Crystallogr.* **14** 617
Lindsay S M, Burgess S and Shepherd I W 1977 *Appl. Opt.* **16** 1404
Morioka Y 1986 *J. Mol. Struct.* **146** 191
Morioka Y and Nakagawa I 1983 *J. Phys. Soc. Japan* **52** 23
Morioka Y, Toriumi K, Ito T, Saito A and Nakagawa I 1985 *J. Phys. Soc. Japan* **54** 2184
Rehwald W 1973 *Adv. Phys.* **22** 721
Saito A, Morioka Y and Nakagawa I 1984 *J. Chem. Phys.* **88** 480
Shapiro S M, Axe D J, Shirane G and Riste T 1972 *Phys. Rev.* B **6** 4432
Vacher R and Boyer L 1972 *Phys. Rev.* B **6** 639
Yoshihara A, Burr J C, Mudare S M, Bernstein E R and Raich J C 1984 *J. Chem. Phys.* **80** 3816
Yoshihara A, Haneda Y, Otake T, Takahashi M, Satoh K, Aizawa K, Suzuki M, Kisara A, Shohji S, Sasaki T and Fujimura T 1990 *Bull. Res. Inst. Sci. Meas. Tohoku Univ.* **39** 71 (in Japanese) at press
Yoshihara A, Haneda Y, Shimada Y and Fujimura T 1989a *J. Appl. Phys.* **66** 328
Yoshihara A, Satoh H, Takahashi M, Yamakami T, Arashi H and Fujimura T 1989b *Ferroelectrics* **96** 167
Yoshihara A, Suzuki T, Yamakami T and Fujimura T 1985 *J. Phys. Soc. Japan* **54** 3376